transecting ACL and MCL ligaments. Nanoparticles were administered intravenously to rats (n = 3) 3 weeks after the surgery (i.e. early OA) at dose of 2.7 mg/Kg Fe (48 μmol/Kg Fe). T1 (TE/TR: 13/1250 ms) and intermediate T2-weighted (TE/TR: 25/2000 ms) MRI were acquired at 20 min and 3 h after injection, utilizing a 9.4T in-vivo micro-MRI. Bone adaptations after surgery were imaged using in-vivo micro-CT.

Results: Nanoparticles with average diameter of 16 nm ± 5.95 and spherical shape were obtained. Successful conjugation of BP to SPIONs was concluded by observing amide and phosphonate peaks on FT-IR spectroscopy as well as detection of elemental phosphorous by XPS technique. Bone-targeting nanoparticles showed 65% binding to HA in-vitro, with 95% of them remaining bound after 24 h. SPIONs exert their effects by reducing T2 value and to a lesser degree T1. In-vivo MRI revealed 'negative enhancement' at regions of active remodeling as early as 20 min following SPIONs-ALN injection, definable as dark hypointense band of decreased signal on T1 and T2 weighted MR sequences (Fig.). The areas of greatest 'negative enhancement' included the growth plates (which are open and active sites of bone turnover in rats throughout life), the tibial and femoral subchondral bone, and the femoral trochlear groove, which is a region known to later develop osteophytes in this animal model. Enhancement remained present 3 hours after injection.

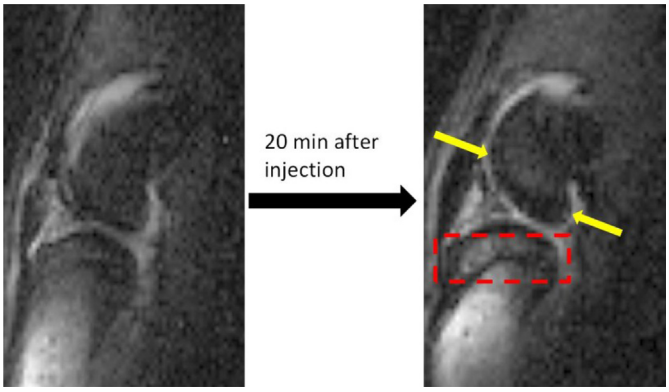

Fig. Intermediate. T2-weighted fat-suppressed MRI: Sagittal plane showing 'negative enhancement' of the joint (medial) at femoral trochlear and condylar subchondral bone (arrows) as well as the growth plate (red box), with dark bands developing after SPIONs-ALN injection.

Conclusions: This study successfully detected altered bone turnover in the early stages of an animal model of OA, particularly at subchondral bone, long before it becomes sclerotic. This approach is the first report on imaging of bone remodeling using MRI. The current approach can potentially produce images of bone remodeling similar to radioactive 99mTechnetium MDP bone scan, with greater spatial resolution, no ionizing radiation, and the opportunity to also assess cartilage integrity on the same study. The conjugative strategies presented here may serve as a novel platform of non-ionizing dynamic bone imaging tracers, capable of detecting bony adaptations prior to their radiological manifestation, with potential for earlier diagnosis of OA.

454
CHARACTERIZATION OF EARLY CARTILAGE DEGENERATION ASSOCIATED WITH ANTERIOR CRUCIATE LIGAMENT INJURY USING T1-RHO MAPPING MAGNETIC RESONANCE IMAGING

K. Okazaki, K. Osaki, H. Matsubara, H. Mizu-uchi, S. Hamai, Y. Iwamoto. *Kyushu Univ., Fukuoka, Japan*

Purpose: Anterior cruciate ligament (ACL) deficiency is known to be correlated with cartilage degeneration of the affected knees. However it is not fully understood what area of cartilage within the joint surface would be affected by the harmful effects of instability due to the ACL deficiency. In addition, there might be a different pathology in the cartilage damage between the effect at the event of ACL injury in acute phase and the subsequent repetitive instability in chronic phase. The purpose of this study was to characterize the early degenerative changes of articular cartilage associated with ACL deficiency, focusing on the location of the cartilage damage within the joint and the influence of the duration after the injury. We analyzed the cartilage denature in ACL deficient knees using T1rho mapping MRI, which can evaluate the content of proteoglycans within the articular cartilage.

Methods: The subjects consist of 39 patients with ACL injury (age: 27.5 ± 10.2) and 14 healthy controls (age: 37.1 ± 6.0). The patients were divided into two groups: 22 patients for group A (acute group) who had been examined within 12 weeks after the injury, and 17 patients for group B (chronic group) examined after 12 weeks from the injury. On the sagittal MR images at the medial and lateral compartment, 3 regions of interest (ROI) on the femoral condyle and 2 ROIs on the tibial plateau was defined in the cartilage area, respectively, as follows: The most distal point on the femoral condyle along with the axis of femoral shaft was identified as the point of 0°. The ROIs was defined as 45° anterior from 0° ("anterior area"), 45° posterior from 0° ("middle area") and from 45° posterior to 90° ("posterior area"). The ROIs in the tibial cartilage was defined by dividing the cartilage into two areas as anterior and posterior. The mean T1rho values within the ROI was measured.

Results: At the medial compartment, the T1rho value was significantly higher in group B (chronic) compared to the controls at the femoral middle area. There was no significant difference between either group A and B or group A and controls. At the lateral compartment, group B showed significantly high T1rho values in the femoral anterior area compared to the controls, while group B did not show significant differences compared to either controls or group B. Because group B showed more variations of the values at most of ROIs compared to the controls or group A, the group B was further divided into two subgroups based on whether the duration after the injury was more or less than 2 years (subgroup B1 and B2, respectively). The T1 rho value was significantly higher in subgroup B2 at the anterior and medial are of femoral condyle than either that in subgroup B1, group A or the controls. At the lateral compartment, the value in subgroup B1 was significantly higher in the anterior area of the femoral condyle than that in the controls. Additionally, the presence of meniscus injury was correlated with the higher values at the middle area of medial femoral condyle in group B compared to that in controls.

Conclusions: This study suggests that the degenerative change of articular cartilage occurs as the time passed after the injury. The area in which the degenerative change likely occurs is on the medial femoral condyle that contact with the tibia in a relatively low angle of flexion, 0 to 45 degrees. At the lateral femoral condyle, more anterior area would be involved in chronic phase. This might be associated with the repetitive anterolateral rotatory instability. It was also suggested that the risk of cartilage degeneration increase after 2 years from the injury. The presence of medial meniscus tear is associated with the cartilage damage of the medial femoral condyle in chronic phase.

455
A NEW METHOD TO MEASURE TRABECULAR BONE TEXTURE ON HAND RADIOGRAPHS: DATA FROM THE OSTEOARTHRITIS INITIATIVE

M. Wolski, P. Podsiadlo, G.W. Stachowiak. *Curtin Univ., Perth, Western Australia, Australia*

Purpose: Grading of hand radiographs for joint space narrowing and osteophytes is the traditional method for assessing hand OA. However, this assessment can be difficult and inaccurate since the changes of cartilage volume in finger joints are small, the grading requires experienced readers to be reproducible and there is no sensitivity to early OA. Thus, a new hand OA assessment method is required. A solution could be in the applications of fractal analyses of finger bone texture regions selected on hand radiographs. The reasons are that the bone texture changes in early stages of OA, it exhibits fractal nature and it is related to 3D bone structure. However, currently there is no method that could quantify accurately small size bone regions on hand radiographs. We have developed a new method, called augmented variance orientation transform (AVOT) method, to measure the roughness and directionality of small texture regions at individual scales.

Methods: The AVOT method calculates the fractal signatures (FSs) in different directions. FS is a set of fractal dimensions (FDs) calculated at individual image sizes (i.e. scales) while FD is a measure of texture roughness. High value of FD means a rougher texture. The method allows for the analysis of hand bone texture regions that are small in size and selected on arbitrarily oriented fingers. Initially we evaluated whether our method can accurately differentiate between computer generated isotropic and anisotropic fractal texture images of sizes ranging from 20 × 20 to 64 × 64 pixels. This is because roughness and anisotropy of bone texture changes with OA. These sizes correspond to those found on hand radiographs. Isotropic textures had FDs varying from 2.1 to 2.9 in steps of 0.1

(400 images per FD), while anisotropic textures had dominating directions of 120° and 30° (400 images per direction). For those images, three parameters at scales ranging from 2 to 7 pixels (depending on image size) were calculated, i.e. FS along the direction of the texture roughest part (FS_{Sta}), aspect ratio (StrS) and direction signatures (StdS), respectively. The aspect ratio and direction measure the texture anisotropy. We also evaluated our method for its sensitivity in differentiating the bone texture between subjects with and without radiographic hand OA. The subjects were taken from the Osteoarthritis Initiative (OAI) public use data set (OAI Datasets 0.2.2 and 0.C.1). Images from centre A were used since they exhibit smallest size amongst the five centres (150 DPI). This strategy allows for testing "the worst scenario", i.e. 20 × 20 pixel regions. We used 20 pairs of subjects (n = 20, 14 women) with (OA cases) and without (controls) OA in the 5th distal interphalangeal (DIP5) joint. OA was defined as: (i) joint space narrowing (JSN) grade 2 or worse, (ii) osteophyte grade 2 or worse, or (iii) JSN grade 1 with an osteophyte grade 1. These criteria approximate Kellgren and Lawrence (K/L) grade 2 or worse. The case-control pairs were individually matched by sex, age, body mass index and race. For each hand x-ray, 20 × 20 pixels bone texture regions were selected on the distal and middle phalanges adjacent to the DIP5 joint (Fig. 1). For each bone region, the FS_{Sta}, StrS, StdS parameters were calculated at scales of 0.34 and 0.51 mm. One-way analysis of variance ANOVA with Tuckey HSD (Games-Howell if appropriate) post hoc tests and paired samples t-tests (Wilcoxon signed-rank tests if appropriate) were used ($p < 0.05$ is significant).

Results: For all image sizes and scales, values of FS_{Sta} were statistically significantly different between isotropic fractal images. StrS values obtained for anisotropic surfaces were lower than those for isotropic surfaces, and StdS agreed with the dominating directions. Compared to the controls, OA middle phalanges exhibited significantly lower FS_{Sta} at sizes 0.34 and ($p = 0.018$) and 0.51 mm ($p = 0.021$), and higher StrS at 0.34 ($p = 0.015$) and 0.51 mm ($p = 0.002$). In the distal phalanx, FS_{Sta} at size of 0.34 mm ($p = 0.044$) was lower for OA cases than controls.

Conclusions: The AVOT method can differentiate between small isotropic and anisotropic fractal textures, and also between finger bones with and without radiographic OA. Although further large-scale studies are still required, our results show the potential of the method for the quantification of OA changes in the finger bone structure.

Acknowledgments: This research was supported by Australian Research Council's Discovery Early Carrier Research Award (project number DE130100771).

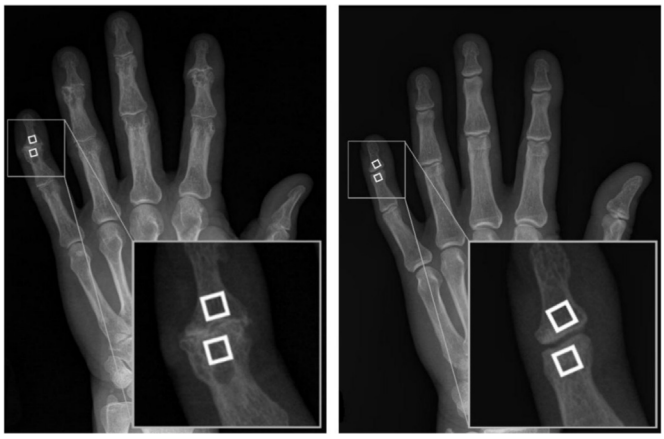

Fig. 1. X-rays of hands (*left*) with and (*right*) without radiographic OA in the DIP5 joint. White squares are bone texture regions selected.

456
QMRI-BASED RISK FACTORS FOR SYMPTOMATIC KNEE PAIN: DATA FROM THE OAI

J.G. Tamez-Pena †,‡, J. Farber ‡, J. Galvan-Tejada †, E. Schreyer ‡, V. Treviño †, P.C. Gonzalez ‡, S. Totterman ‡. † *ITESM, Monterrey, Nuevo Leon, Mexico;* ‡ *Qmetrics Technologies, Rochester, NY, USA*

Purpose: Chronic knee pain is a common feature of osteoarthritis (OA); the pain may be associated with different risk factors and may have various etiologies. The purpose of this work was to determine which MR imaging characteristics can be used as risk factors - or imaging biomarkers - for the subsequent development of symptomatic knee pain.

Methods: Right knees from an Osteoarthritis Initiative (OAI) cohort with untreated right knee pain were examined. This medication free cohort had right knee pain symptoms recorded as "Pain most days of a month in past 12m" (RKSX = 2) on observations later than the 12 month visit (V01). At the screening visit (P1), the 12 month visit (V01) control subjects had lower symptomatic scores (RKSX = {0,1}). A control group with no right knee pain was matched for age, BMI, gender and no therapy. Only subjects with DESS MRI images were analyzed. The MRI DESS analysis was done by Qmetrics technology software that automatically segmented the femoral, tibial and patellar cartilage into several regions of interest (ROI): femur, tibia, patella, central medial femur, central lateral femur, medial tibia, lateral tibia, medial trochlea, lateral trochlea, medial patella, lateral patella. Automated segmentations that failed to correctly segment cartilage tissue were removed from the analysis. Each ROI was quantitated for volume, area, thickness, curvature and DESS signal contrast properties. ROI Statistical descriptors were computed for thickness, curvature and contrast. Using the control subjects, all measurements were adjusted for BMI, age and gender differences. The measurements then were z-transformed using the rank inverse normal transform. Finally, all measurements were categorized as low-control-quartile ($p < 0.25$), mid-control-range (0.25 to 0.75) and top-control-quartile ($p > 0.75$). The time to pain event (RKSX = 2) on cases and the time of last observation were used in Cox-Survival-Models. A bootstrapped-step-wise feature selection algorithm based on the Integrated Discrimination Improvement (IDI) was used to extract a robust multivariate COX-survival model from the 12 month observation (V01). The COX-model categorized subjects into high risk and low risk to develop future knee pain. All models were internally validated using a 10-fold cross-validation. Furthermore, the risk model was tested in the baseline observation and the 24 month observation.

Results: 80 cases qMRI (39:41 Males:Females), with successful right knee segmentations were included. 194 qMRI analysis (87:107 Males:Females) were used as controls. The total population had an average age of 62.9 ± 9.5 years and BMI of 27.0 ± 4.4. There was no statistical difference between study subjects and controls for BMI and age. Table 1 shows the six MRI features that separate subjects into high/low risk for the development of chronic pain at the three starting points. The femur curvature was a consistent risk factor: Odds ratio (OR) 1.92 (1.5 to 2.5). Also constant predictive was the bone-cartilage signal contrast of the lateral femur: 2.42 (2.0 to 2.85). Figure 1 shows the Kaplan-Meier plots of the Baseline, 12 Month and 24 Month visits.

Conclusions: Abnormal curvature of the femur and low DESS signal contrast at the lateral femur articular surface are risk factors for the development of knee pain. Although the casual relationship of these findings with the evolution of OA still has to be established, this fact may be used to make clinical and treatment decisions for the prevention of symptomatic knee pain.

Table 1
qMRI-based risk factors for Symptomatic Knee Pair. (−) low quartile, (+) at top quartile.

Feature	Cases mean (std)	Control mean (std)	One Year Odds Radio (95 Cl)	Baseline Odds Ratio (95 Cl)	Two Year Odds Ratio (95 Cl)
Femur Curvature (Trimmed)	0.040 (0.006)	0.041 (0.006)	1.92 (1.51 to 2.50)(-)	1.64 (1.25 to 2.13)	1.36 (1.13 to 1.69)
cLF Superficial Contrast (5%)	−37.10 (1.236)	−3.918 (1.185)	2.42 (2.02 to 2.85)	1.74 (1.38 to 2.25)	1.89 (1.58 to 2.30)
Tibia Deep Layer Contrast (std)	1.154 (0.129)	1.116 (0.113)	0.52 (0.27 to 0.89) (−)	0.95 (0.60 to 1.50)	1.19 (0.60 to 2.15)
Lateral Trochlea Curvature (Trimmed)	0.029 (0.007)	0.029 (0.005)	1.73 (1.40 to 2.18) (+)	1.34 (1.09 to 1.65)	1.36 (1.11 to 1.71)
Femur Superficial Contrast (Mean)	2.281 (0.665)	2.607 (0.514)	3.27 (1.92 to 5.61)	2.07 (0.86 5.08)	1.23 (0.62 to 2.31)
Femur Curvature (Mean)	0.030 (0.006)	0.032 (0.005)	0.21 (0.09 to 0.49)	0.75 (0.39 to 1.37)	0.60 (0.26 to 1.22)